In press for "Sea Surface Sound '94"
(Ed. M. Buckingham)
Presented by T.G. Leighton, UCLA, California
in March '94

Study of bubble fragmentation using optical and acoustic techniques

T. G. Leighton, M. F. Schneider and P. R. White
Institute of Sound and Vibration Research, University of Southampton, Highfield, Southampton SO9 5NH, UK

The predictions of a theory of bubble fragmentation (Longuet Higgins 1992) are compared with experimental results. The theory, which models the fragmentation event as the simultaneous insertion of a number of randomly positioned dissecting planes through a cubical air body to predict the number and size of daughter bubbles produced can be formulated in one, two, or three dimensions, corresponding to the mutually perpendicular directions of the plane normals. The lower-dimensional events being more amenable to visual observation, the fragmentation of a nominally two-dimensional bubble (a 'disc' of air) was studied and found to be most accurately modelled by the one-dimensional theory. Subsequent high-speed video observation did indeed reveal one-dimensional characteristics in the collapse, though it found that it deviated from theory in that the dissecting planes are neither randomly positioned nor inserted simultaneously. The fragmentation of three-dimensional bubbles was studied by exploiting their acoustic emissions. Use of a Gabor transform in a time-frequency representation (TFR) of hydrophone data gave a time of formation and the natural frequency of each bubble entrained in a small freshwater waterfall, and also revealed the presence of a low-frequency cloud mode which had to be eliminated from subsequent comparison with theory. Once again the best fit was obtained for the model which utilised only one-dimensional fragmentation, a result in accord with the geometry of the waterfall. Data obtained through entrainment of bubbles by a liquid jet, impacting a liquid surface from above at various angles, could not be fit simply by the theory. The dimensionality of the best fit varied with the flow rate in, and angle of, the jet, suggesting more than one type of entrainment could operate. This was further indicated by multi-modal distribution in bubble size obtained at certain intermediate angles. Bi-modal distributions were also obtained using hydrophone data of light rainfall over the ocean on a calm day. Comparison of theory and experiment yields discourse on the differing roles of shape oscillations and surface waves on bubble fragmentation, and the issues involved with incorporating this distinction into the model.

INTRODUCTION

Bubbles may be generated through a number of common processes, all of which relate to changes (formation, rupture, closure, merging etc.) of one or more gas/liquid interfaces. Energy from such processes, channelled through mechanisms involving surface tension, hydrostatic and hydrodynamic forces etc., can generate bubble oscillation and consequently acoustic emission. In 1933 Minnaert[1] produced a

first-order formulation of the natural frequency of a pulsating bubble (neglecting surface tension and viscous effects, and assuming adiabatic behaviour for the gas), which varied inversely with bubble radius. Minnaert compared his prediction with observations of injected bubbles. Further investigations, notably those of Strasberg[2,3] and Devin[4] continued the study, the latter predicting that for the relatively large air bubbles in water employed by Minnaert the pulsations would indeed approach the adiabatic situation. In 1987 Leighton and Walton[5] compared hydrophone data from injected bubbles in a variety of liquid/gas combinations with both the adiabatic theory of Minnaert and the non-adiabatic case. They then employed these relations to obtain from hydrophone data the number and size of bubbles generated in brooks, streams and waterfalls. The observed natural processes involved a number of entrainment mechanisms, ranging from hydrodynamic pressure drops when a stream flows over a rounded stone, to liquid jet and drop impact in a waterfall. In 1992 Longuet Higgins[6] produced an analysis which demonstrated how the problem of predicting the number and size of daughter bubbles might be approached, and compared the theory with the data of Leighton and Walton[5], Toba[7], Updegraff[8] ands Medwin and Daniel[9], noting the dearth of laboratory data. In this study the fragmentation of both 'two-dimensional' (i.e. nominally circular) and 'three-dimensional' (i.e. nominally spherical) bubbles is observed using optical and acoustic techniques respectively, with the entrainment of three-dimensional bubbles including waterfall and ocean rainfall observations. The results are compared to the theory.

I. THEORETICAL MODEL

Longuet-Higgins[6] proposed a model to predict the initial bubble size distributions from entrainment events by statistical analysis where "...the process of entrainment is compared with the splitting of a cubical block by three sets of planes, each set being parallel to a face of the cube, and each set being inserted into the block independently of the others". These randomly spaced planes divide the initial block into a number of rectangular sub-blocks, representing newly formed bubbles. Depending on the form of the entrainment, the block can either be divided by one, two or three sets of planes. In the natural world Longuet Higgins suggested that a one-dimensional break up may occur when water is running over a smooth stone and entrains a cylindrical volume of air. The two-dimensional model considers a cubical block of unit volume which is split by two sets of perpendicular and independent planes. The distributions were calculated using numerical integration. In a similar way the model can be extended to three dimensions, with distributions having a much more negative mean. For comparison of theory and experiment, the dimension and number of planes are chosen to best fit the standard deviation and skewness of the data, and the height of the theoretical curve is adjusted to relate to the total number of bubbles and the bin width.

II. METHODS

A. FRAGMENTATION OF TWO-DIMENSIONAL BUBBLES

A so-called 'two dimensional' bubble (an 'air disc') was formed by injecting an air bubble into degassed water between two plates of polymethylmethacrylate (PMMA) separated by an O-ring. The energy for fragmentation is provided by a repeatable combination of flow and pressure disturbance. The apparatus consists of a U-tube (Fig. 1a), partially filled with degassed water, connected by hose to the PMMA plates (Fig. 1b) at one end and stoppered at the other. The bubble is manoeuvred to the centre of the plates by a magnetic slider, and expands when the vacuum pump reduces the ambient pressure. The stopper is then rapidly opened, and the resulting liquid pressure change causes bubble collapse, which is videoed at 50 f.p.s., 1 ms exposure. The minimum pressure applied to the bubble was approx 10 mbar higher than the vapour pressure of water (p_{min} approx. 20 mbar at 20°C). The pre-expansion and pre-collapse diameters (d_o and d_g) of the bubble, and its daughters, were measured using a graticule magnifying glass. The partial vacuum caused deflection of the plates of about 0.2 mm in the centre and 0.06 mm at the O-ring when the lowest pressure was applied. This deflection was taken into account when the bubble volumes were calculated. The release of the pressure lead to an oscillation of the plates (measured by accelerometer to be at 30 Hz and of 0.5 seconds duration) and an oscillating water flux. Bubbles with radii smaller than the distance between the plates were hemispherical, rather than cylindrical (Fig. 1(c)). Since the third dimension may influence the dynamics of such bubbles significantly more than for the larger air discs, the transitional size between the two is indicated on the results (Fig. 3). All the experiments in terms of bubble distributions were carried out with bubbles placed in the centre of the plate. In general 10 to 30 break-ups of one bubble size at a particular pressure were recorded to get representative histograms of daughter bubbles. The accuracy of the measurement of the bubble volume was $\pm 5\%$.

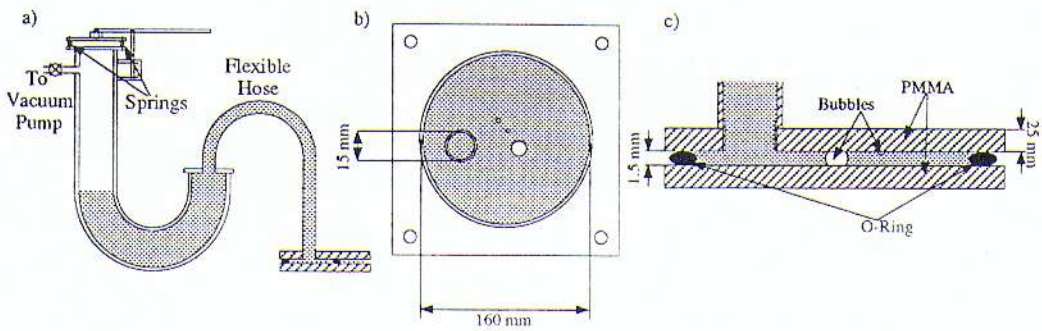

FIG. 1: Apparatus for air disc fragmentation. (a) The U-tube. The PMMA plates viewed from (b) top and (c) side

B. ENTRAINMENT OF THREE-DIMENSIONAL BUBBLES

The entrainment and fragmentation of three-dimensional (i.e. roughly spherical) bubbles was monitored through the use of the passive acoustic emissions, which were analysed to obtain the bubble size distribution. This was first done by Leighton and Walton[5] for the entrainment in babbling brooks and under waterfalls. In that study the time series hydrophone data was visually analysed to determine the presence of the exponentially-decaying sinusoids ('signatures') characteristic of bubble entrainment, the frequency of the sinusoid indicating the bubble size. The present study exploits in essence the same technique, though with additional signal processing to enable bubble counts to be obtained during conditions of low signal-to-noise ratio and high entrainment rates, where there is significant overlap between signatures. The system was automated to enable rapid analysis of large populations.

To construct a time-averaged frequency spectrum from a data source wherein the critical frequency data is invested in the form of transients (such as the underwater sound of rainfall) is clearly to throw away a great deal of information. If there is significant noise present, or if the transients do not repeat, the key information may not be simply modified but submerged altogether. Clearly a better option in such circumstances is to form a time-frequency representation (TFR), where the energy of the data is decomposed as a function of both time and frequency. The nature of the signatures studied here makes the application of the TFR method, based on the Gabor transform, and described in ref. 10 particularly attractive. This method produces a two dimensional set Gabor coefficients, rather than a representation of the acoustic power invested in each frequency band, enabling the bubble signatures to be identified. A routine which thresholds (based the value and gradient of the Gabor coefficients) then automatically counts and sizes the bubbles. Entrainment data was gathered for analysis in this way in a brook, and beneath a water jet which impacts a water surface from above, and in the ocean under calm conditions during light rainfall.

1. In a Brook Waterfall

The acoustic signals of newly entrained bubbles were measured in a brook on the University Campus on 25.05.93. A hydrophone (Brüel & Kjaer 8104) was mounted on a steel rod and placed at 15 cm depth beneath the mean water level in a bubble field created at the base of a small waterfall (height approx. 20 cm, called location A) and at a depth of 10 cm in a different bubble field approx. 30 cm away (location B). The water was running very smoothly over the step. The signal from the hydrophone was amplified with a charge amplifier (Brüel & Kjaer 2635) and recorded on a DAT Recorder (AIWA HHB 1 PRO, with a flat frequency response from 20 Hz to 22 kHz). At both locations approx 10 min of data were recorded. Back in the laboratory the recordings were played back through a lowpass filter (Barr and Stroud EF5/20, roll off approx 48 dB/octave) into a data acquisition box, where they were acquired into MATLAB. The time history of the data showed that the most bubbles occurred in the frequency range between 500 Hz and 2 kHz. During acquisition a sample rate of 10 kHz was used with the lowpass

filter set at 5 kHz (the absence of significant signal components at these frequencies relieved the need for a guard band).

2. Liquid Jet

The experiment was carried out in a 1.8m x 1.2m x 1.2m deep glass reinforced plastic tank which was filled to 1 m depth with water. A hose, terminating in a glass tube (5 mm inner diameter), was mounted near the water surface at varying angles (Fig. 2). The hydrophone (Brüel & Kjaer 8105) was at approx. 300 mm depth beneath the entrained bubbles, but approx. 150 mm off-axis. The signal from the hydrophone was amplified and recorded on the DAT-recorder (as in IIB.1) or acquired directly into MATLAB, via the lowpass filter. A sample rate of 44 kHz and a lowpass filter with a cut off frequency set to 20 kHz were employed.

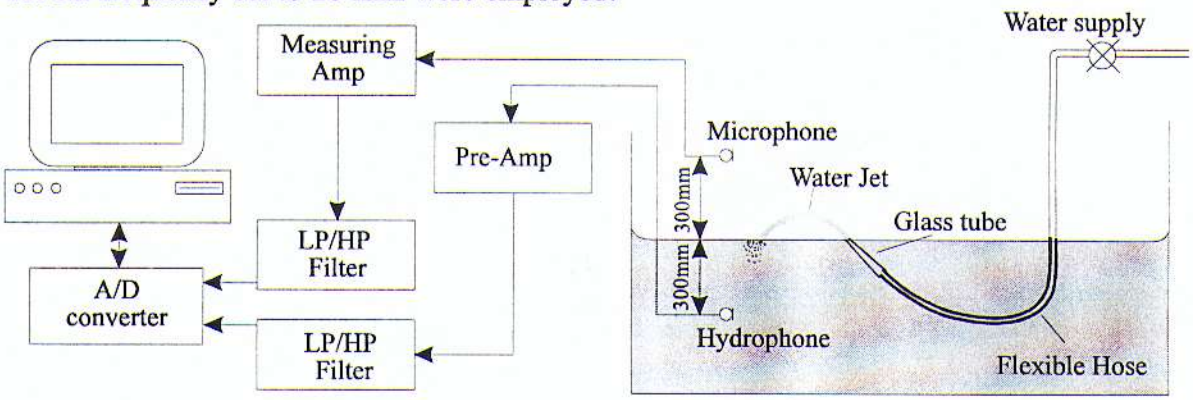

FIG. 2. Apparatus for entrainment by liquid jet.

3. Rainfall Over Ocean

On 11-9-93 an array of four hydrophones (Brüel & Kjaer, three type 8104, and one 8105) was deployed in 27 m of water from a 13 m research vessel in the Solent of the English Channel to the west end of the Isle of Wight (50° 59.962' N, 1° 35.748' W) to measure the underwater sound of light rainfall in the ocean under calm conditions. The hydrophones were mounted on a rigid stabilised rack in a rectangle (1.14 m x 0.5 m) parallel to the sea surface. The rack was mounted on elastic suspension and held by the A-frame of the boat about 2 m from the back of the ship, so that the hydrophones were located in 1 m depth. The hydrophone signals were amplified using 4 charge amplifiers (Brüel & Kjaer 2635) and recorded onto a multi channel tape recorder (Store 7DS Racal) at the a tape speed of 15 i.p.s. in the direct recording mode yielding a frequency range from 100 Hz to 75 kHz. During the measurements the engine was turned off, the wind speed (from the east) was less than 1 m/sec and the water depth was approx 39 m. Due to the movement of the ship in the waves, which subsequently lead to a movement of the hydrophones in the vertical direction as well as through the waves the hydrostatic pressure at the hydrophones changed. This low frequency signal limited the gain on the charge amplifiers, although the high pass filters of the pre-amps were set to 2 Hz. Therefore the signal to noise ratio of the measurements was limited. Back in the

laboratory the signal was acquired into MATLAB by playing the tape back at 1/8 the original speed and sampling at 20 kHz. The data was passed through a band pass filter (Barr & Stroud EF5/20) set to pass frequencies between 100 Hz and 9 kHz. This effectively meant that the data was sampled at 160 kHz and band pass filtered between 800 Hz and 72 kHz. The signal was analysed using the Gabor transform to get the TFR and the bubble count.

III. RESULTS

A. VISUALISATION OF COLLAPSE OF TWO-DIMENSIONAL BUBBLES

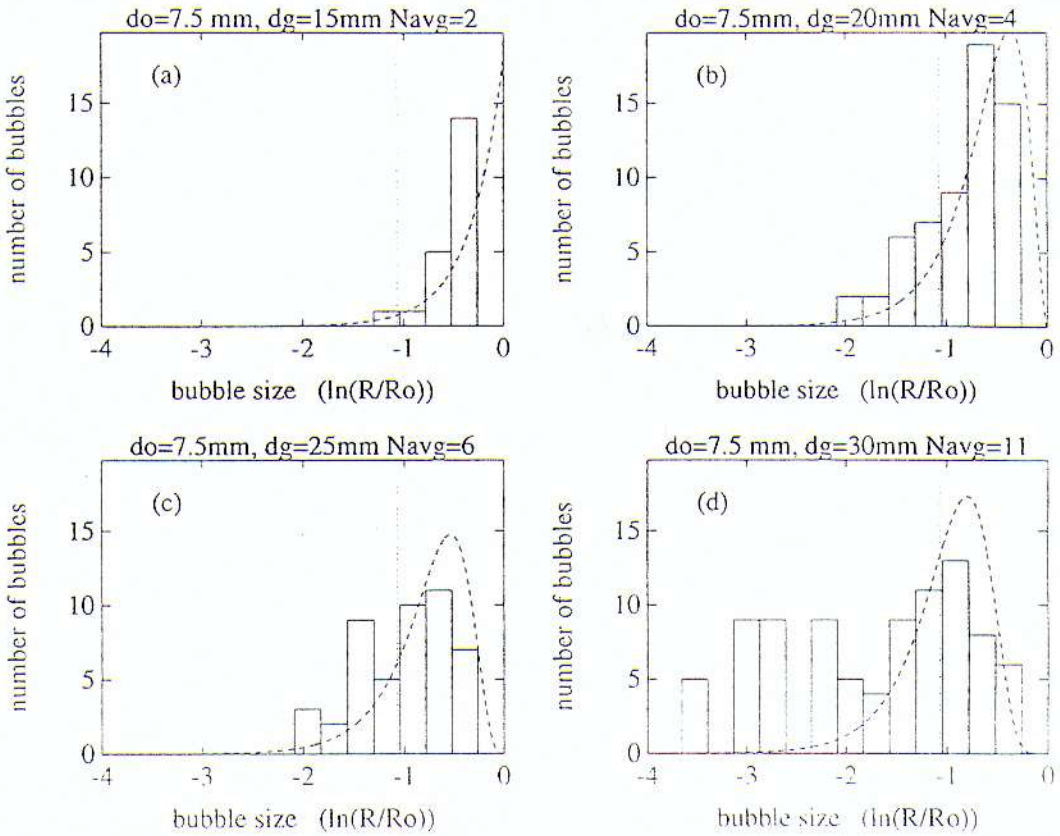

FIG. 3. Histograms of the distribution of daughter bubbles after break-up for an air disc of initial diameter d_0=7.5 mm for different excitation energy with the best fitting theoretical curves. The dotted vertical line shows the transition where the measured radii smaller than this are less than the distance between the plates.

Results are presented in Fig. 3 for the fragmentation of a bubble following the application of different pressure reductions (as indicated in the figure by the varying values of d_g, the diameter of the air disc when fully expanded), the bubble having a diameter of d_0=7.5 mm prior to expansion. The applied pressure reduction, and consequently the subsequent pressure step, were increased from the value required to just cause fragmentation. When a small pressure difference between applied pressure and atmospheric pressure was released, giving low excitation energy the bubble was split into

two daughter bubbles. For higher excitation energies more splitting occurred and more bubbles were created. The dependence of bubble size was also investigated. For bubbles with bigger diameters the pressure release lead to an increased number of daughter bubbles when the same pressure difference was applied. The bubble distributions however, show that for high excitation most of the daughter bubbles have radii smaller than 1.5 mm and do not strictly confirm to the intended "air-disc" approach, as they are smaller than the thickness of the plate gap. The data in Fig. 3 is compared with the theory. The measured diameters of the cylinders were converted into radii of spheres R with the same volume. Depending on the average number N_{avg} of daughter bubbles per break the best value of m with the appropriate curve was fitted.

The best fit to the data always occurs when the one-dimensional theory for fragmentation is applied (D=1). In Fig. 3(a) the average number of daughter bubbles is $N_{avg} = 2$. The best fit is given by the one-dimensional theory with D=1, m=1 shown as the dashed line in Fig. 3(a). The theoretical curve does not fit to the measured data, because no very big daughter bubbles were observed. This suggests that the preferred splitting occurred towards the middle of the bubble. This would give a more narrow distribution than would the random splitting as assumed in the theory, which would give rise to additionally both very small and very large daughter bubbles. In Fig. 3(b) the excitation energy was increased leading to an increased number of daughter bubbles. The mean of this distribution is more negative than predicted by the theory resulting from a preferred splitting in the middle of the bubble. The theoretical distribution with D=1, m=3 and N_{avg}=4 (shown as the dashed line in Fig. 3(b)) gives the best fit. Fig. 3(c) shows a similar distribution but with a more negative mean and less peaked when the applied pressure difference is increased, creating more daughter bubbles. Again the theoretical curve for a splitting in one dimension D=1 with an increased number of planes m=5 (N_{avg}=6), shown as the dashed line in Fig. 3(c), fits much better than the two- or three-dimensional theories. Increasing the excitation energy further leads to more daughter bubbles as shown in Fig. 3(d) where most of the bubbles have radii smaller than the transitional size shown by the dotted vertical line. It is therefore not surprising that no single theoretical curve fits the entire data in Fig. 3(d), since the processes involved in the fragmentation of hemispherical and cylindrical bubbles would be expected to differ. However the figure shows the theoretical curve for D=1, m=10 which fits reasonably well for the cylindrical bubbles in the distribution.

The results suggest that the bubbles were not broken randomly by sets of planes from two directions, but it seemed that the splitting occurred only in one direction with the plane inserting near the centre of the bubble to give a narrower distribution. This hypothesis is confirmed using high speed video pictures taken from the break up of bubbles having pre-expansion diameters of d_0=7.5 mm (for pre-collapse diameters d_g see caption). In Fig. 4(a), when the pressure is released the upstream wall involutes and forms a jet which travels across the cavity to impact the downstream wall (frame 2). This leads to the splitting of the bubble (frame 3), forming two daughters of approximately equal size (frame 4). These smaller bubbles undergo severe distortion from the circular shape and move with the water flux in the direction of the connector, which can be seen

by comparing frame 3 and frame 4. With the higher excitation energy the smaller bubbles develop jets in a similar way and are split into further smaller bubbles, which is influenced by the movement of the plates and the associated water flux, and the rebound of the pressure wave (frame 6). The bubbles move due to the flux of the water around them (frames 7 and 8) and change their location and their shape for as long as 500 ms (this time is identical to the time the PMMA-plates oscillate). All of the daughter bubbles present at the end of the experiment were formed between frame 5 and frame 7. A variety of fragmentation behaviours was seen in other collapses, including the simultaneous formation of two jets (parallel (Fig. 4(b)) and perpendicular (Fig. 4(c))). Collapses (a) and (c) differ primarily through slight differences in initial bubble shape.

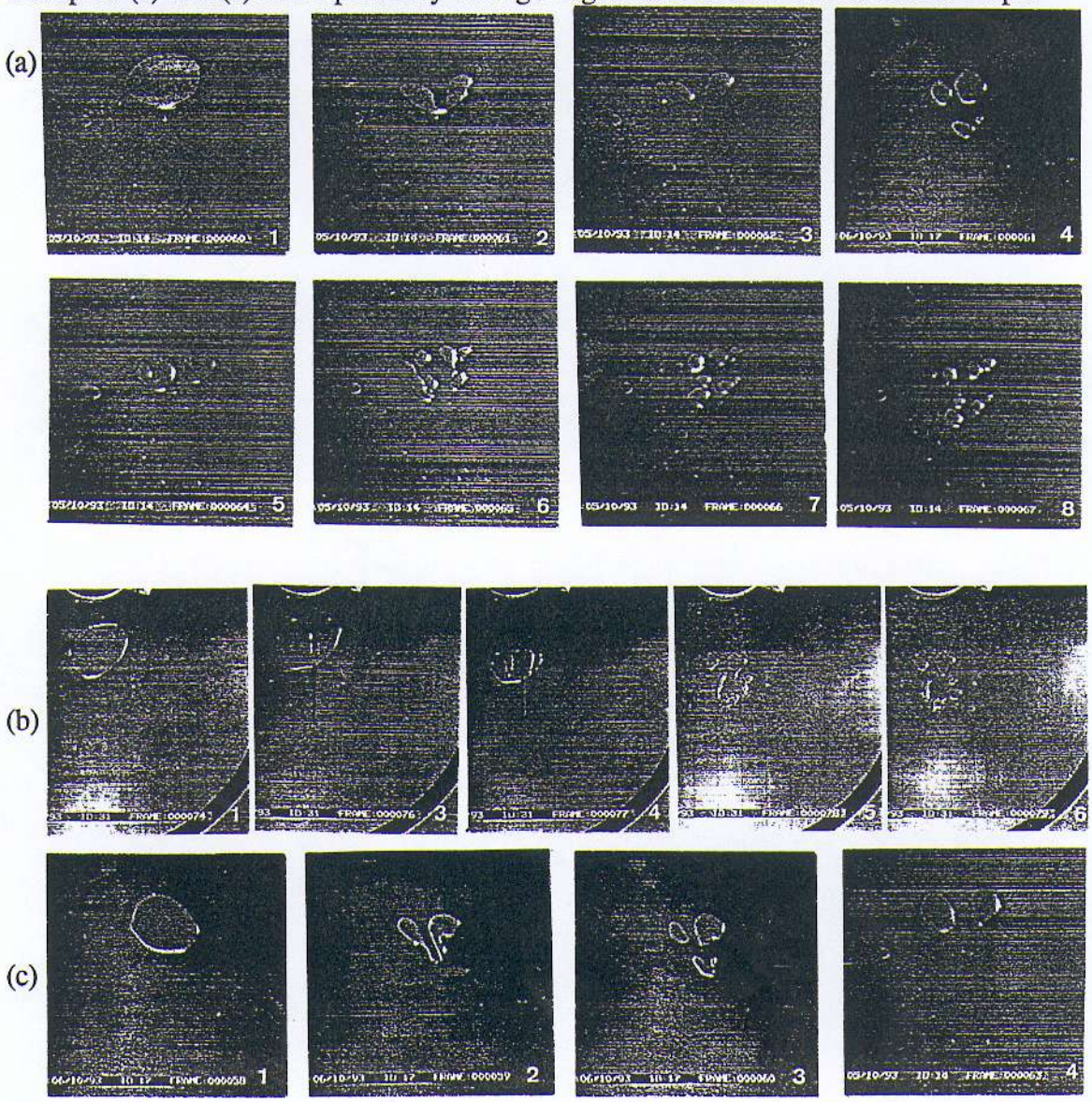

FIG. 4. (a) Successive video prints (20 ms interframe ; d_0=7.5 mm) of fragmentation. (a) (d_g=20 mm) Frame 1: shortly after pressure release, bubble has lost its initially circular profile. (b) (d_g=25 mm) Two parallel (right jet arrowed), and (c) (d_g=20 mm) two perpendicular, jets fragment bubbles. cm rule on left of frame. Frame height : (a) 60 mm (b) 100 mm (c) 60 mm.

B. ACOUSTIC OBSERVATIONS OF ENTRAINMENT OF THREE-DIMENSIONAL BUBBLES

1. In Brook Waterfall

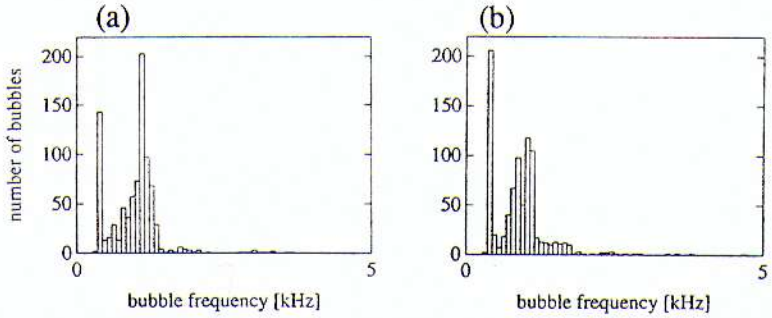

FIG. 5.
Bubble resonance distributions (50 s of brook data each): (a): location A. (b) location B. Time-frequency representation used 128 point Fourier transforms; and damping coefficient of 100 [s^{-1}].

Bubble size distributions were obtained (Fig. 5). The distributions at both sites show two distinct peaks, the first at 400 Hz and the second at 1.2 kHz, can be detected. At site A (Fig. 5(a)) the hydrophone was near to a bubble field having a frequency distribution from 700 to 1300 Hz, whereas at site B (Fig. 5(b)) the hydrophone record was dominated by the component at around 400 Hz. For such a system to entrain a large number of bubbles of size resonant around 400 Hz (equivalent to radius R_0=7.5 mm) is anomalous for a number of reasons. The distribution is not smooth in this region which, whilst not being unphysical, is unusual. More telling is the failure to observe such large bubbles visually. Large bubbles were observed on the water surface, but their number was significantly smaller than shown in the distributions. In addition examination of the time history of signals with a frequency content of 400 Hz, showed decaying sinusoids, yet their amplitude was in general smaller than would be expected from large bubbles, and the decay was not monotonic, but rather an amplitude modulation featuring waxing and waning. If this were due to large bubbles, such an effect might arise through shape oscillation[11]. However the bubble size is rather large for significant mode coupling. The most likely explanation is that the low frequency component was due to a cloud mode[12,13], excited by bubble oscillation (note that some large bubbles were observed, and their entrainment oscillations would resonate with the cloud mode), turbulence or impact sounds. The signal would therefore be regarded as transients in the TFR and counted in as newly entrained bubbles. The 400 Hz component, not being the result of bubble entrainment, is eliminated prior to the statistical analysis to allow comparison with the theory. The best fit to data (Fig. 6) is found for a one-dimensional collapse (D=1, m=∞). The curves seem not to fit well, although the best fit theoretical curve obtained by the statistical parameters is chosen. The theoretical curves are not so peaked and do not have a standard deviation as small as the measured curves. Comparing the time-history with the theory shows that the bubbles are entrained sequentially, rather than simultaneously, so that the data must be considered as summed distributions if comparison with theory is to compare like with like.

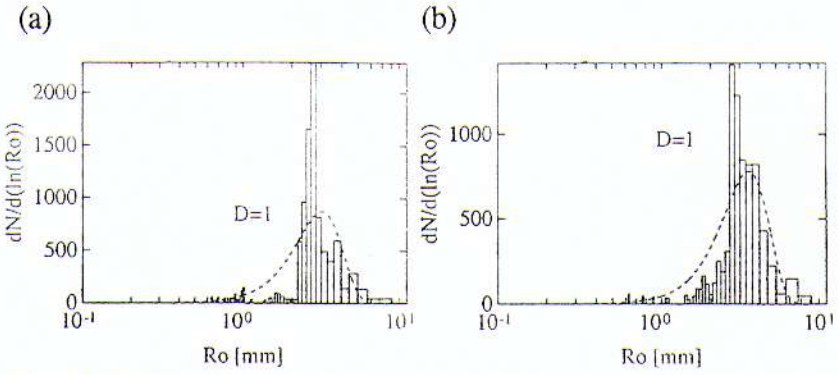

FIG. 6.
Measured bubble radius density distributions for brook data from Fig. 5, at (a) site A, (b) site B, with theoretical curve for D=1 and m=∞.

2. Liquid Jet

The time history contained individual bubble events of four types: an ideal decaying sinusoid; an oscillation with beats; a high frequency oscillation superimposed upon a low resonance frequency emission; and an oscillation which has a growing amplitude for the first few cycles and then decays away. Similar types have been observed under laboratory breaking waves[11]. Fig. 7 shows 0.5 s of the time history of the hydrophone and of a microphone placed in air 300 mm above the location of bubble entrainment. Each bubble detected by the hydrophone has a counterpart in the microphone signal. Through expanding the time scale a time delay, due to the lower sound speed in air, can be detected. The microphone signal shows a clear peak at the moment of entrainment, but the signal is much weaker and the oscillation decays away much faster. Furthermore in the trace of the microphone signal sometimes an oscillation was detected with no associated output at the hydrophone. It is believed that this signals were due to bubbles bursting at the surface, producing a 'plop' with associated surface waves.

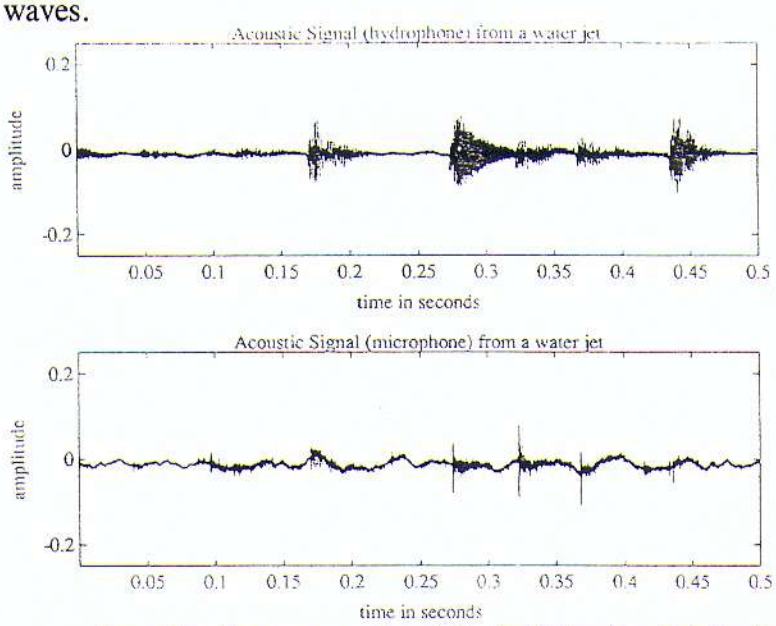

FIG. 7. Hydrophone and microphone signals from bubble entrainment by water jets

Investigation was made of the bubble size distribution obtained when a water jet strikes the surface of the water and entrains bubbles. This can be seen in terms of a one-dimensional bubble break up, as Longuet Higgins predicted, which may have arisen from

the splitting up of a column of air entrained by the jet. The jet angle and flow rate were varied. A minimum jet speed was needed to entrain bubbles. When the jet speed was lower no entrainment occurred, with one exception: small surface waves on the water tank disturbing the water jet caused bubble entrainment. These surface waves were caused by entrained bubbles which rose to the `surface by buoyancy. The maximum jet speed employed was limited to ensure that no subsequent splashes occurred. During the experiment it became clear that for large angles of incidence the main reason for entrainment was the disturbance of the water surface by bubbles rising to the surface. For smaller angles the water jet carried the entrained bubbles away from the jet and the waves on the tank surface set up when the bubbles burst did not affect the water jet.

Fig. 8 shows three distributions from an experiment with a constant water flow (approx. 3 l/min) and various the angles from surface to glass tube (80°, 60°, 30° shown) in increments of 10°. As the angle was reduced the number of bubbles entrained per time interval decreased initially and then began to increase again, this is as one would expect. All the obtained distributions showed a peak at 700 Hz, which could again be influenced by bubble cloud oscillations and had a maximum at approx. 2 kHz. Some of the distributions showed a second peak at about. 5 kHz, suggesting that a second entrainment mechanism was involved. Comparisons made between the obtained distributions and theory showed no real agreement. The measured distribution for 80° was narrow and fitted to the one-dimensional model (for D=1 and m=∞), whereas at small angles (50°, 40°, 30°) the distributions are broader and are better modelled by the two-dimensional theory. In between the bubble density showed several peaks with a very broad distribution.

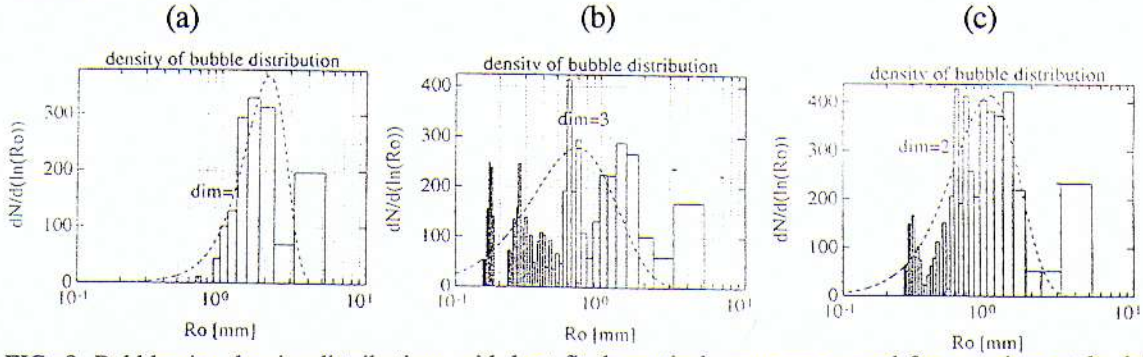

FIG. 8. Bubble size density distributions with best fit theoretical curves measured for entrainment by jet in a water tank for 5 s. Jet flow rate 2.5 l/min. Surface-to-nozzle angle: (a) 80°; (b) 60°; (c) 30°.

Measurements were also made for constant angles of 55° (0.3-1.6 l/min) and 70° (0.5-3.2 l/min) and for a water jet perpendicular to the surface, all with varying flow rates. The number of bubbles entrained increased with increasing flow. Two peaks became evident in the distribution of bubble frequencies, one at 700 Hz and a smaller peak at around 2 kHz which increased with increasing water flow. The theoretical curves did not fit to the measured distributions, partly because two peaks were observed. The time histories again demonstrated sequential, rather than simultaneous, events.

3. Rainfall over the Ocean

The distribution of bubble size for the individual hydrophones is shown in Fig. 9. Two peaks can be detected in all four frequency distributions: a dominant one at about 14 kHz and a smaller one at 5 kHz. The shapes of several other distributions obtained at different times showed all the same peaks. The distribution from hydrophone 1 and 4 show a dominant peak at 5 kHz whereas the distributions from hydrophone 2 and 3 have their dominant peak at 14 kHz. A possible explanation of these different distributions might be due to the location of the hydrophones: Hydrophones 1 and 4 were on the long side of the rectangular array closest to the ship, and their recordings will have been influenced by bubbles produced by gentle waves lapping against the side of the ship.

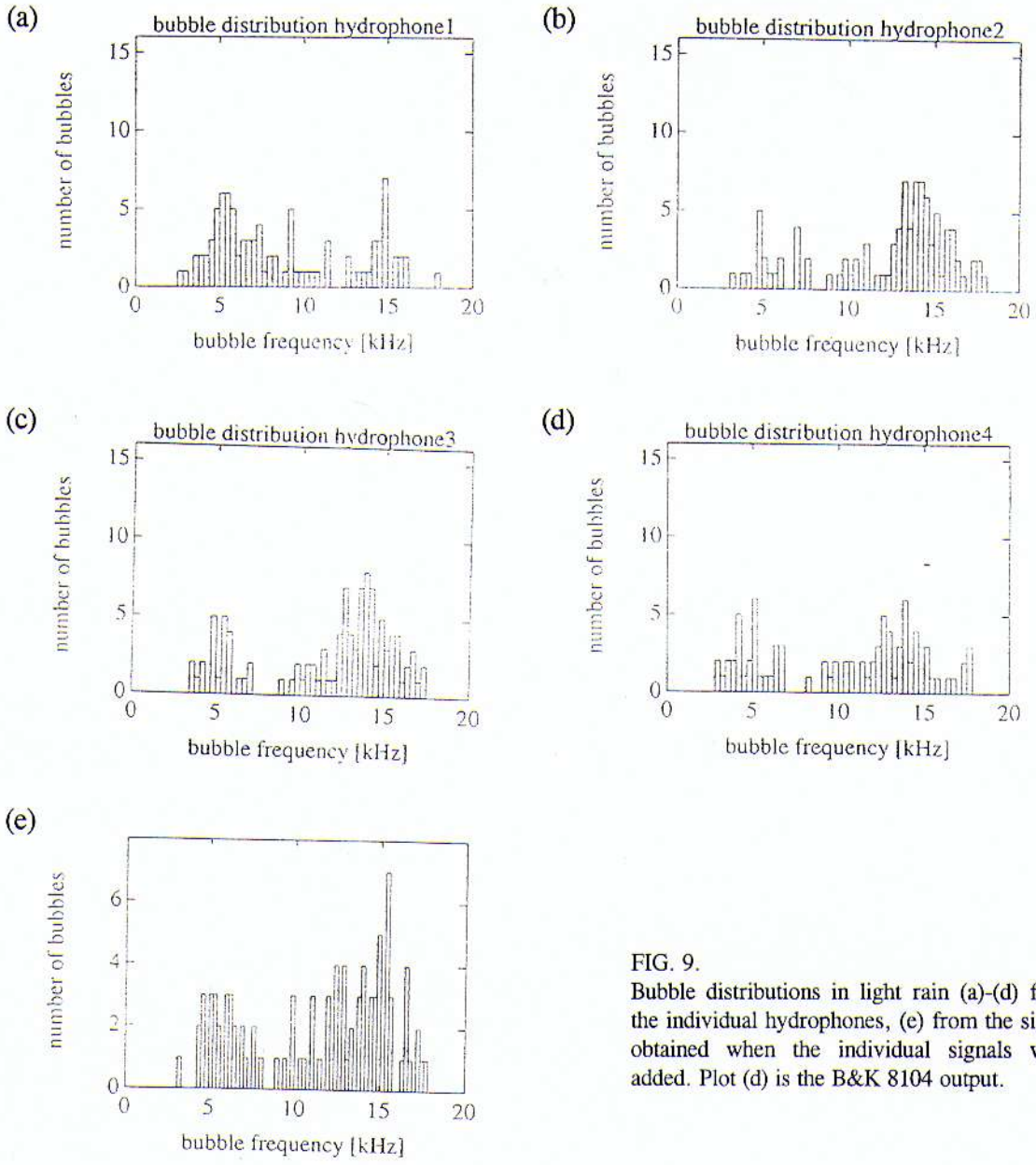

FIG. 9.
Bubble distributions in light rain (a)-(d) from the individual hydrophones, (e) from the signal obtained when the individual signals were added. Plot (d) is the B&K 8104 output.

The signals of the four hydrophones were added, providing directionality towards the centre of the rectangle which they formed. The added signal was then analysed, with the resulting bubble count exhibiting a dominant peak at 15 kHz (Fig. 9(e)).

IV. DISCUSSION

The observations reveal a number of features encountered in these entrainment situations which differ from the model. Observations of two-dimensional bubbles suggest that the planes are not necessarily inserted either sequentially or at random positions, but rather at sites related to the modes of shape oscillation of the bubble. The lower-order modes are preferred, and since these would give rise to insertions which divide the bubble into a number of similarly-sized regions, a dominance of this type of plane insertion would tend to reduce the number of very small or very large daughters (i.e. similar to the size of the original bubble) produced. However bubble fragmentation need not simply occur through mass participation of the air body as a single oscillator: daughter bubbles which are very much smaller than the original can form from surface waves on the bubble, the wavelength of which is much smaller than the bubble radius (Ref. 15, Figs. 4.26 and 4.31). Such activity can produce a large number of very small bubbles without significantly affecting the size of the original bubble. This raises an interesting question: if we model this as the simultaneous insertion of a large number of planes, the resulting daughter count is of a large number of smaller bubbles, and a single large bubble. However, if the planes are considered to be inserted sequentially, the final bubble count is of a large number of small bubbles (the same as for the previous count) but a number of large daughters equal to the number of insertions. This is because the large bubble remaining after the separation of each small daughter is counted at each insertion. This flaw in such a system of counting is manifest when one considers that, observing at the end of the fragmentation series, one would physically see a single large bubble and a number of much smaller daughters.

The following seems the most feasible protocol. Fragmentations associated with the low-order shape modes of the bubble planes should be considered to occur sequentially: The only dissecting planes which may be inserted simultaneously must be all those associated with a single mode during a single collapse cycle of the shape oscillation. Consider the one-dimensional collapse illustrated in frames 1 to 5 of Fig. 4(a), where a bubble is bisected by a jet the position of which is determined by a second order ($n=2$) oscillation (frames 2), and the same fate befalls the resulting two daughters (frame 5) (a process which will produce four fragments from a single bubble). The description entails the insertion of a single plane associated with the $n=2$ oscillation on three occasions (once in the original bubble, and then once in each of its two daughters). Had however the original bubble been fragmented by a third-order ($n=3$) shape oscillation (Fig. 4(b)), the model would have employed simultaneous insertion of the two parallel planes associated with the $n=3$ mode, to produce three daughter bubbles. If each of these had then been fragmented by a third-order mode, the

model would have incorporated this by the simultaneous insertion of the two parallel planes appropriate to n=3 through one of the daughters, then through the second, and lastly through the third. The result would have been a population of nine daughters. Clearly even for insertion in one dimension, the question of which planes are inserted simultaneously and which are inserted sequentially is involved. However one simplification that may be found in nature is that fragmentation by the second-order mode may be far more common than by modes of higher order (Ref. 15, Figs. 2.17, 3.29-3.31). In contrast, the form of fragmentation which involves the production of daughters from surface waves, rather than shape modes, is most suitable modelled by the simultaneous insertion of planes. Unlike the shape modes, where in the low orders the planes are inserted at positions well within the body of the bubble as dictated by the order of the mode to produce a number a similar-sized daughters, in fragmentations associated with surface waves the planes are inserted preferentially close to the bubble extremes, to generate a large number of very small daughters and a single much larger one.

The observation that a one-dimensional fragmentation theory best fits the data in a number of situations is not surprising. In some circumstances it will be influenced by the dominance of the low-energy second-order shape oscillation, compared with those of higher order: such fragmentations are necessarily the insertion of a single plane from one direction only. In other situations it will be influenced by the local environment determining a unique direction, the physical definition of which will influence the mechanisms to promote uni-directional processes. Such definition might occur through the geometry of the water flow (for example, in a water fall), the direction of propagation of a pressure wave or flow (as in the case of the fragmentation of circular bubbles described above), or through the proximity of (Ref. 15, Fig. 4.29) or coalescence with (Ref. 15, Fig. 4.19) another bubble. In sequential processes, such as is illustrated in Fig. 4(a), whilst the conditions of the pressure pulse and flow no doubt contribute to defining a unique direction and so influencing the two daughter bubbles to undergo one-dimensional collapses in frame 5, so too will the preceding one dimensional collapse (frame 2) contribute to that definition.

V. CONCLUSIONS

The theoretical predictions for the number and size of daughter bubbles produced by the break-up of a cubical air pocket have been compared with data obtained both visually and acoustically from a range of entrainment processes. These include the collapse of two-dimensional 'circular' bubbles under pressure fluctuations and flow, and the entrainment of three-dimensional 'spherical' bubbles by waterfalls, liquid jets and rainfall. The Gabor transformed proved to be particularly useful in obtaining population information from data containing noise and overlapping bubble signatures.

Certain of the entrapments observed in this study involve processes that do not immediately appear to follow the modelled fragmentation of a self-contained air body.

All except the fragmentation of the 'air disc' involve, to a greater or lesser extent, a surface which, to a first approximation, is planar and 'infinite', the disturbance of which causes closure and detachment and therefore the entrainment of some daughter bubbles. Whilst subsequent break-up of these bubbles would more closely fit the model, how accurately the free-surface event is described by the theory depends on details of the closure and detachment processes, which clearly differ significantly between entrainment by plunging jet and by light rain. Nevertheless the theory does fit in several cases, and it is the fact that the analysis is a first attempt to model the entrainment process, and is unencumbered by the sophistications outlined above which would make it more closely describe the bubble fragmentations visualised in this study, which give it the versatility to approach such widely differing entrainment processes.

ACKNOWLEDGEMENTS

The authors wish to acknowledge the support of the Natural Environment Research Council (SIDAL 00670) also to Prof. R Roy for his assistance in the construction of the rig to deploy the hydrophones for the rainfall studies. We also wish to thank A. Phelps and J. Fackrell for their help during this work.

[1]Minnaert M. (**1933**). "On musical air-bubbles and sounds of running water," *Phil. Mag.* 16, 235-248
[2]Strasberg M. (**1953**). "The pulsation frequency of nonshpereical bubbles," *J.Acoust.Soc.Am.* **25**, 536-537
[3]Strasberg M. (**1956**). "Gas bubbles as sources of sound in water," *J.Acoust.Soc.Am.* **28**, 20-26
[4]Devin C.(**1959**). "Survey of thermal, radiation and viscous damping of pulsating air bubbles in water," *J. Acoust. Soc. Am.* **31**, 1654-1667
[5]Leighton T.G., Walton A.J. (**1987**). "An experimental study of the sound emitted from gas bubbles in a liquid," *Eur. J. Phys.* **8**, 98-104
[6]Longuet-Higgins M.S. (**1992**). "The crushing of air cavities in a liquid," *Proc.R.Soc.Lond.* **439**, 611-626
[7] Toba Y (**1961**). "Drop production by bursting air bubbles on the sea surface (III). Study by use of a wind flume," *Mem. Coll. Sci. Kyoto* A **29**, 313-343
[8] Updegraff G. (**1989**). "In situ investigation of sea surface noise from a depth of 1 meter," PhD, University of California at San Diego, U.S.A.
[9]Medwin H. and Daniel. (**1989**). "Acoustical measurements of bubble production by spilling breakers," *J. Acoust. Soc. Am.* **88**, 408-412
[10]Friedlander B. and Porat B. (**1989**). "Detection of Transient Signals by the Gabor Representation," *IEEE Trans. Acoust., Speech, Signal Processing* **37**, 169-180
[11]Longuet-Higgins M.S. (**1990**). "Bubble noise spectra," *J. Acoust.Soc.Am.* **87**, 652-661
[12]Prosperetti A. (**1985**). "Bubble-related ambient noise in the ocean," *J. Acoust. Soc. Am.* 78 (Suppl), S2
[13]Carey W. (**1985**). "Low frequency ocean surface noise sources," *J. Acoust. Soc. Am.* 78 (Suppl), S1-2
[14]Medwin H., Beaky M. (**1989**). "Bubble sources of the Knudsen sea noise spectra," *J.Acoustic.Soc.Am.* **86**, 1124-1130
[15]Leighton T.G. (**1993**), *The Acoustic Bubble*, Academic Press, London
[16]Leighton T.G., Fagan K.J. Field J.E. (**1991**). "Acoustic and photographic studies of injected bubbles," *Eur. J. Phys.* **12**, 77-85